Available online at www.sciencedirect.com
SCIENCE DIRECT®
Journal of Magnetic Resonance 161 (2003) 15–24
JMR Journal of Magnetic Resonance
www.elsevier.com/locate/jmr

# Single excitation multiple image RARE (SEMI-RARE): ultra-fast imaging of static and flowing systems

A.J. Sederman,* M.D. Mantle, and L.F. Gladden

*Department of Chemical Engineering, University of Cambridge, Pembroke Street, Cambridge CB2 3RA, UK*

Received 31 May 2002; revised 10 October 2002

**Abstract**

This paper describes the development and application of a new rapid, full **k**-space acquisition imaging pulse sequence based on the rapid acquisition with relaxation enhancement (RARE) methodology. We have termed this pulse sequence single excitation multiple image RARE (SEMI-RARE). We demonstrate the application of SEMI-RARE to the visualisation of a static liquid phantom and it is shown that up to 120 images can be acquired from a single excitation. By exploiting the inherent relaxation and diffusion contrast within the series of images, the SEMI-RARE provides an ultra-fast method for characterising the spatial distribution of chemical species and phases within complex systems. The pulse sequence is then applied to the study of single- and two-phase flow in a single narrow tube of inner diameter 2.9 mm. In particular, it is shown that 8 two-dimensional slice-selective images for two-phase bubble-train flow in a single tube can be acquired from a single excitation at effective echo-times of 37, 109, 181, 253, 325, 397, 469, and 541 ms. The visualisation enables the determination of gas/liquid bubble sizes and velocities during two-phase flow. We also report the first direct evidence, obtained from magnetic resonance measurements, of liquid re-circulation zones associated with bubble-train flow. The robustness of the SEMI-RARE technique makes it an attractive fast imaging technique for the study of multi-phase flow phenomena, which are often characterised by large variations in magnetic susceptibility, and are of widespread interest in chemical engineering.


*Keywords:* RARE; Fast imaging; Multi-phase flow; Bubble-train flow

## 1. Introduction

Spin-echo based rapid imaging techniques such as RARE [1] are extremely useful when high image quality is required in samples exhibiting a broad range of magnetic susceptibilities. RARE imaging and its variants turbo (TSE) and fast (FSE) spin echo have found a multitude of applications in medical imaging but there are few reports [2–4] of fast imaging-based protocols able to address problems encountered in chemical and process engineering in which, typically, the increase in range of magnetic susceptibilities, shorter nuclear spin relaxation times and more rapid timescales over which the system is changing impose far greater requirements on the imaging pulse sequence than those found in medical systems. Here we report the development of a new RARE-based imaging pulse sequence and demonstrate its application to single- and two-phase bubble-train flow in a single narrow tube or 'capillary.' A detailed understanding of the liquid-phase hydrodynamics in two-phase bubble-train flow in similar sized capillaries [5,6] is an important consideration when dealing with heat and mass transfer in certain reaction engineering problems.

Rapid **k**-space sampling strategies have recently been reviewed by Hennig [7], in which a detailed discussion of the relative merits of EPI- and RARE-based imaging sequences are presented. Moreover, the author identifies considerations with respect to implementation of these fast imaging techniques with particular reference to flowing systems. Nearly all applications employing fast imaging techniques such as EPI and RARE acquire at best a single two-dimensional image following a single radio-frequency (r.f.) excitation pulse. Bosmans et al. [8] have reported a two image (termed in their paper as

* Corresponding author.
*E-mail address:* ajs40@cam.ac.uk (A.J. Sederman).

1090-7807/03/$ - see front matter © 2003 Elsevier Science (USA). All rights reserved.
doi:10.1016/S1090-7807(02)00141-6

'dual-echo,' and named double-echo HASTE, or DE-HASTE) half **k**-space turbo spin echo HASTE [9,10] sequence which acquires two images from a single excitation pulse at different effective echo times, to characterise liver lesions.

The imaging sequence reported in this paper describes how a new variant of the RARE sequence yields multiple images from full **k**-space data at multiple echo times following a single r.f. excitation. We have termed this sequence single excitation multiple image RARE (SEMI-RARE). In addition to the technical description of SEMI-RARE we show its applications to a multi-component static system, and then single- and two-phase flow in a single narrow tube of inner diameter 2.9 mm. For the case of single-phase flow, the SEMI-RARE sequence is shown to yield the parabolic flow profile expected for flow in the laminar flow regime. The ability to obtain the parabolic flow profile confirms that there is no mis-registration of interfaces visualised in successive images as a result of the finite time required for data acquisition. Images of two-phase, bubble-train flow are then reported; data are shown for equal gas and liquid flow rates of $4\,\mathrm{ml\,min^{-1}}$. This system was selected since it was not only of direct relevance to systems we are studying with application to reaction engineering (e.g., flow within ceramic monolith catalysts [11]) but also because such dynamic two-phase systems are particularly challenging for existing magnetic resonance visualisation strategies as the system is not in steady state and hence the boundaries and regions containing signal are constantly moving. In particular, when the system is not in steady state and contains relatively fast-moving boundaries, it is not possible to use a method that allows for significant $T_1$ relaxation between multiple excitations because of the associated displacement of the boundary over the relatively substantial imaging time compared to the time-scale of motion of the boundary. It is noted that magnetic susceptibility effects at the air–water interface (and associated short $T_2^*$ of $\sim$1 ms) eliminate the possibility of using a gradient recalled EPI-based imaging sequence in such applications. However, the SEMI-RARE sequence, with effective image times of 37 ms after excitation for the first image and at subsequent intervals of 72 ms, provides a first opportunity to investigate such a system.

The SEMI-RARE technique reported here provides significant advantages over other MRI techniques in the study of magnetically heterogeneous samples as a result of its ability to achieve high temporal/spatial resolution in combination with high signal-to-noise data acquisition. The magnitude of the signal acquired may be close to $M_0$, the equilibrium magnetisation, for images acquired shortly after excitation by allowing full $T_1$ relaxation before the beginning of the sequence. In contrast, FLASH [12] and SSFP [13] can achieve temporal resolution similar to the SEMI-RARE technique but suffer from relatively poor signal-to-noise and have $T_2^*$ signal attenuation. However, SEMI-RARE has the disadvantage of only being able to acquire images for the duration of the signal coherence. Phase shift or phase contrast velocity imaging methods [14] suffer from poorer temporal resolution and typically poorer signal-to-noise compared to SEMI-RARE. In particular, the phase shift or contrast velocity imaging methods require two images to be acquired that differ in the magnitude of the velocity weighting gradient. This is not possible in the study of unsteady two-phase flow where the system (and $B_0$ heterogeneity) will change between successive image acquisitions. Of course, over a longer acquisition time the phase shift approach can be used to produce a high quality, quantitative image of steady state single-phase flow. As stated earlier, EPI fast imaging techniques are not suitable for systems with short $T_2^*$ and though PEPI [2] overcomes this drawback, the lack of a phase rewind gradient can produce artefacts associated with pulse angle imperfections. While the use of composite pulses in the implementation of PEPI has been shown to reduce these artefacts to some extent [4], SEMI-RARE is found to be more robust in application to the study of the multi-phase flow systems reported here.

In this study, SEMI-RARE images from a single excitation are reported for three systems: (i) 120 images of a static water/octanol/glycerol phantom, (ii) 16 images of single-phase flow of water within a narrow tube, and (iii) 8 images of two-phase (air–water) flow within the same narrow tube. Factors determining the number of successive images that may be acquired from a single excitation are the values of $T_2$ and $T_1$, and the extent of diffusive attenuation in the images; the latter effect increasing with higher spatial resolution in the acquired image and hence larger magnitude of the applied field gradient. For both single- and two-phase flowing systems, a further factor limiting the number of images that may be acquired is the residence time of the fluid within the r.f. coil and velocity-related attenuation predominantly associated with the non-ideality of the 180° refocusing pulse [15]. For the case of a two-phase flowing system, additional loss of signal intensity arises from liquid recirculation phenomena within a liquid slug.

## 2. Experimental

The SEMI-RARE pulse sequence is an extension of a standard RARE [1] experiment and is shown in Fig. 1. All pulse and delay timings used in the analysis of the experimental data (see Eq. (1)) are defined in the schematic of the r.f. pulse sequence shown in Fig. 1. $^1$H images were recorded on a Bruker DMX 300 MHz spectrometer operating at a $^1$H frequency of 300.13 MHz. A 15 mm birdcage imaging coil was used

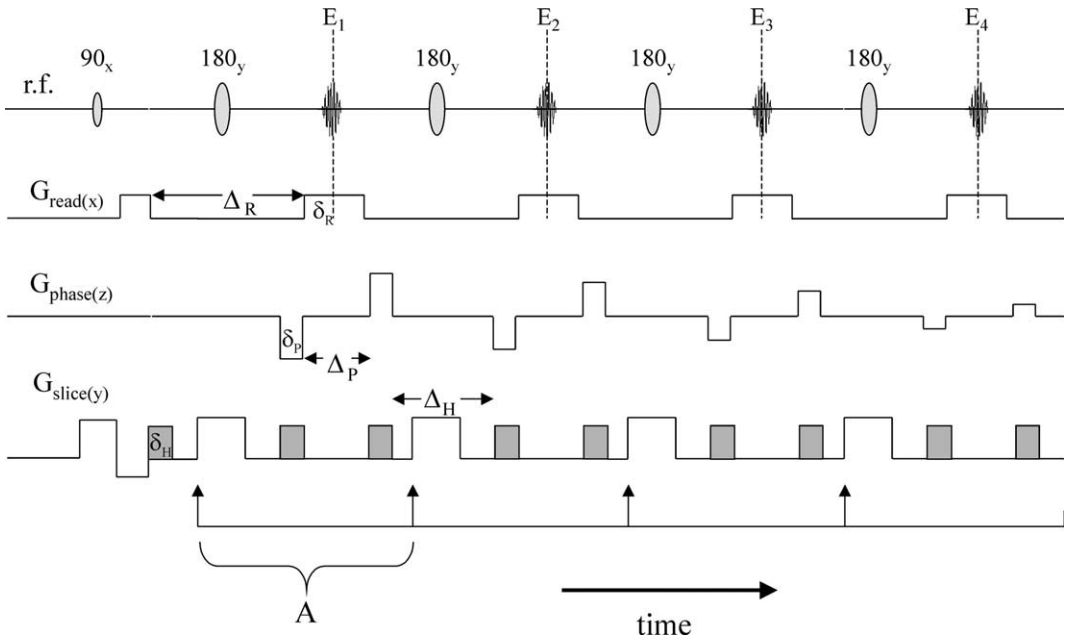


Fig. 1. Schematic showing the timing of the r.f. and gradient pulses during the SEMI-RARE sequence. Shaded gradient areas represent homospoiling gradients. Also shown on the diagram is the definition of $\Delta$ and $\delta$ pulse sequence parameters for the read, phase and slice gradients. Four loops of the SEMI-RARE sequence are shown. To produce n images from a single r.f. excitation, the series of phase gradient pulses identified in the loop A is repeated $n \times r$ times, where $r$ is the number of phase increments per image.

with approximate axial length 35 mm. Spatial resolution was achieved using a 3-axis shielded gradient system capable of producing a maximum gradient of $100\,\mathrm{G\,cm^{-1}}$ in each of the $x$, $y$ and $z$ directions.

### 2.1. Static liquid phantom

The static liquid phantom comprised of a sample tube of internal diameter 23 mm containing water, into which two NMR tubes of inner diameter 9 and 8 mm filled with glycerol and octanol, respectively, were placed. The SEMI-RARE pulse sequence was used to acquire 120 images with an isotropic field of view of 40 mm and resolution of $64 \times 32$ pixels in the read and phase direction, respectively, yielding an in-plane pixel resolution of $0.625 \times 1.25$ mm (Fig. 2). The image slice thickness was 4 mm, obtained using a sinc-shaped 180° pulse. The effective echo time, $T_{\mathrm{eff}}$, for the first image was 34.8 ms. Subsequent images up to a maximum $T_{\mathrm{eff}}$ of 8.1 s were acquired at increments in $T_{\mathrm{eff}}$ of 67.5 ms. The effects of relaxation and self-diffusion contrast on the series of acquired images is clearly observed, and the quantitative nature of the data obtained following corrections for relaxation and diffusion contrast is considered.

### 2.2. Single- and two-phase flow in a narrow tube

Images of both single-phase liquid and two-phase gas–liquid flow were acquired using the SEMI-RARE pulse sequence. A single, narrow Perspex tube (length 2.50 m, i.d. 2.9 mm) was fed through the vertical bore of the magnet. A syringe pump (Harvard Pumps, maximum capacity 560 ml) was used to pump water through the tube. For both case studies the in-plane resolution of the images presented is $64 \times 32$ pixels with a field-of-view of $15 \times 30$ mm; the image slice thickness was 500 μm. Since the RARE sequence is particularly prone to attenuation due to velocity in the read direction but is much less susceptible to flow artefacts in the phase direction [15], the phase direction was chosen to be in the direction of superficial flow. The slice plane was in the $xz$ direction, through the centre of the tube.

In the case of single-phase flow, liquid flow through the tube was visualised for a liquid flow rate of $8\,\mathrm{ml\,min^{-1}}$, corresponding to an average superficial velocity of $20.2\,\mathrm{mm\,s^{-1}}$. The SEMI-RARE sequence was used to acquire 16 images from a single r.f. excitation. The effective echo times for these images were 37 ms for the first image with increments of 72 ms for all subsequent images. The region of the tube through which visualisations were acquired was selected at approximately 350 tube diameters from the inlet so that fully developed parabolic flow was established. In addition to demonstrating the ability of the SEMI-RARE sequence to acquire 16 images from a single excitation, the quantitative nature of the visualisations is considered by exploring the extent to which the data confirm the theoretically predicted parabolic flow profile expected under these experimental boundary conditions.

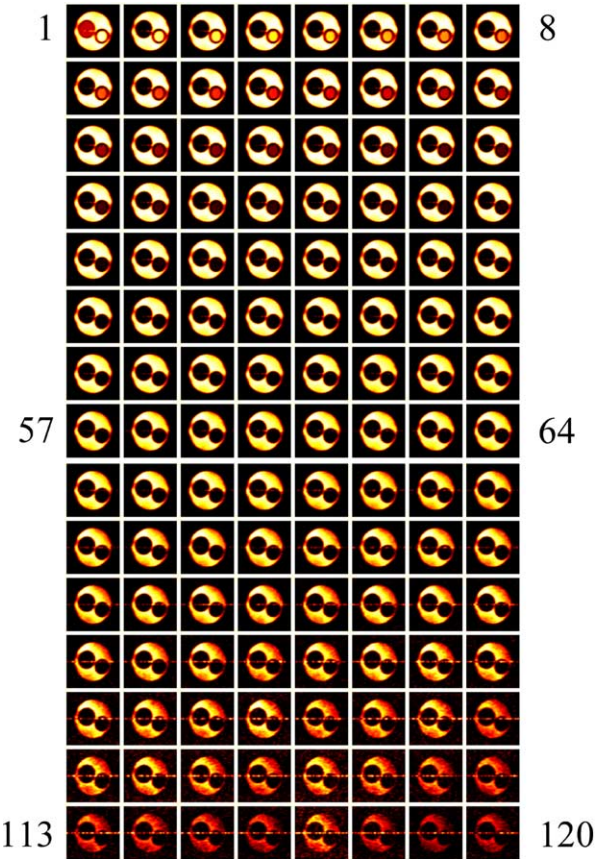


Fig. 2. 120 transverse (*xy*) $^1$H images of the water/octanol/glycerol phantom using the SEMI-RARE sequence. The signal from octanol and glycerol are seen to attenuate more quickly due to their shorter $T_2$ values.

For two-phase flow studies, the gas (air) flow was controlled from a high-pressure air line. The pressure was first reduced to 2 barg and then controlled with a needle valve in series with a calibrated gas flow rotameter. The liquid slugs and gas bubbles were formed by mixing the fluids at an inverted Y-piece mixer of internal diameter 2 mm at both the liquid and gas inlet. Primary control of liquid slug/gas bubble size was achieved by controlling the ratio of the liquid and gas flow rates. Two-phase liquid flow within the tube was established in the form of bubble-train flow with approximately equal gas and liquid flow rates of 4 ml min$^{-1}$. A series of experiments were performed in which 8 images were acquired for each excitation at effective echo times of 37, 109, 181, 253, 325, 397, 469, 541 ms.

### 2.3. Gating-level procedure

For both the single- and two-phase flow imaging studies, the acquired images are gated in order to perform the subsequent analyses. The method used for gating the images employs a gating level at the mid-point of the signal intensity distribution determined from the image, i.e., at the mid-point between the maximum signal and noise levels. Maximum signal and noise levels, and therefore gating levels were calculated separately for each image. For the case of single-phase flow, this analysis was implemented such that for each image a separate gating level was identified for each radial position within the tube. This is necessary when two effects are present in the images: (i) there is a gradual transition between noise and maximum signal level in the image—in the single-phase flow images considered here, this transition occurs over typically 5 pixels; and (ii) there is significant radial variation in signal intensity within an image—clearly, in the case of single-phase flow, radially-varying velocity contrast will exist across the tube. For the case of two-phase flow, the transition between noise and maximum signal levels is much sharper and this additional step in the data analysis is not required.

## 3. Results and discussion

### 3.1. Phantom of non-flowing liquid

Fig. 2 shows 120 transverse images of the water/octanol/glycerol phantom acquired from a single excitation using the SEMI-RARE pulse sequence. It is clearly seen in Fig. 2, that there is signal above the noise level from the water in all 120 images; i.e., for data acquisition times up to 8.1 s after the initial r.f. excitation. Signal from the $^1$H nuclei in glycerol and octanol reduces to the noise level after fewer images due to their shorter effective transverse relaxation times.

The series of images shown in Fig. 2, shows that the SEMI-RARE pulse sequence can be used directly to discriminate between different species and, potentially, phases in a multi-component system, by exploiting the inherent effects of relaxation contrast and diffusion contrast on the signal intensities of the acquired images. It is also possible to correct, at least in part, for the effects of relaxation and diffusion contrast in the images when the system under study allows acquisition of a sufficient number of images following the initial excitation. For completeness, corrections for relaxation and diffusion contrast are considered here for the static liquid phantom. Using the SEMI-RARE pulse sequence, inherent $T_1$ effects for recovery of the initial magnetisation are not relevant, but the magnitude of $T_1$ will influence the effective $T_2$ characterising the system. These effects have been considered in detail by earlier workers [16,17]. Here, we consider only an approximate correction for relaxation time effects and diffusion contrast to demonstrate that the relative importance of these corrections can be identified readily from the SEMI-RARE data and that the ratio of $^1$H spin density values within the image and absolute

values of the $T_2$ of species present are recovered to better than 10%.

An effective relaxation time for the species contained within each pixel in the image is obtained by fitting the decrease in signal intensity associated with that pixel throughout the series of images obtained. All decay curves obtained in this way fitted well to a single exponential. By performing the analysis over several pixels containing each species, average values of 1600, 520, and 29 ms for the water, octanol and glycerol, respectively, were obtained. It is stressed that this does not represent a quantitative $T_2$ analysis. The reasons for this are two-fold. First, diffusive attenuation and hence additional contrast within the images arises due to the application of a magnetic field gradient. Second, the imperfect refocusing of the *nominally* 180° r.f. refocusing pulse will introduce a proportion of $T_1$ relaxation while the magnetisation is in $z$-storage, thereby increasing the observed decay time constant. Despite, any shortcomings of this correction, the ratio of $^1$H spin density relative to water obtained from this analysis by averaging signal intensity in zones A, B and C (A:B:C) identified in Fig. 3b is 1:0.964:0.950 which is in good agreement with the true ratio of 1:0.978:1.03.

The effect of diffusion contrast on the images has been estimated by following the analysis reported by Peters and Bowtell [18] with the addition of a phase gradient term and assuming a pure 180° pulse, to give the following expression for the signal attenuation, $A$, for the $n$th echo in the series:

$$A = \exp\left(\frac{-\gamma^2 D G_R^2}{3}(2\delta_R^3 + 3\Delta_R\delta_R^2)\left(r\left(n-\frac{1}{2}\right)\right)\right) \times \exp\left(\frac{-\gamma^2 D G_P^2}{3}\frac{r(r/2+1)(r+1)}{6}(2\delta_P^3 + 3\Delta_P\delta_P^2) \times\left(n-\frac{1}{2}\right)\right)\exp\left(\frac{-\gamma^2 D G_H^2}{3}(2\delta_H^3 + 3\Delta_H\delta_H^2) \times\left(r\left(n-\frac{1}{2}\right)\right)\right), \quad (1)$$

where $\gamma$ is the gyromagnetic ratio, $D$ is the diffusion coefficient, $n$ is the image number, $r$ is the number of phase increments per image, and $G_R$, $G_P$, $G_H$, are the gradient strengths in the read, phase and homospoil (slice) directions, respectively. All timings are as defined in Fig. 1. The signal attenuation due to diffusion in the experiment reported here was calculated taking parameter values of: $\Delta_P = 800\,\mu s$; $\Delta_H = 984\,\mu s$; $\Delta_R = 1304\,\mu s$; $\delta_{P,H} = 160\,\mu s$; $\delta_R = 400\,\mu s$; $G_R = 7.83\,G\,cm^{-1}$; $G_P = 7.83\,G\,cm^{-1}$; $G_H = 4.70\,G\,cm^{-1}$; $D_{water} = 2.3\times\ 10^{-9}\,m^2\,s^{-1}$; $D_{octanol} = 1.4\times10^{-10}\,m^2\,s^{-1}$; and $D_{glycerol} = 1.8\times10^{-12}\,m^2\,s^{-1}$. The pulse and delay times were those used in the experiment and the values of self-diffusion coefficient were obtained from the literature [19]. Following corrections for the effect of diffusion contrast, the apparent $T_2$ of water increases to 2100 ms. The percentage attenuation attributable to the effect of diffusion contrast for octanol was 1% and much less than that for glycerol and hence attenuation due to diffusion has negligible effect on the apparent $T_2$ values of these species determined directly from the image intensities. The $T_2$ values of the

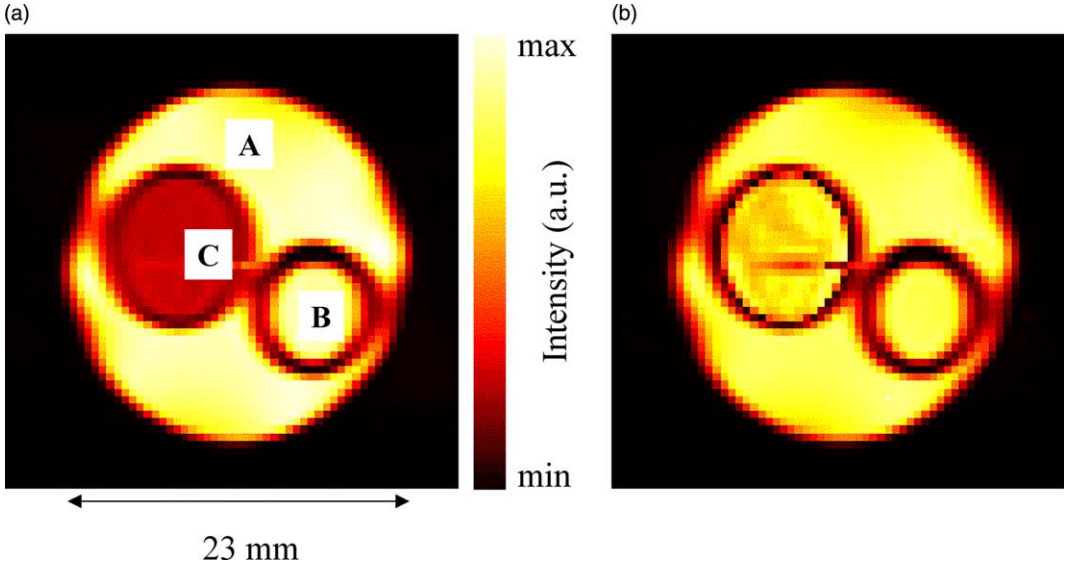


Fig. 3. (a) First image acquired following initial excitation (Fig. 2, Image 1); the phantom comprises a large tube containing water (A) and two smaller tubes containing octanol (B) and glycerol (C). (b) 'Effective $T_2$'-corrected spin density image of the data shown in (a). The $T_2$ values of the species as measured by a CPMG sequence were 1900, 480 and 29 ms for water, octanol and glycerol, respectively. The $T_1$ values determined using an inversion recovery sequence were 2900, 890 and 300 ms, for water, octanol and glycerol, respectively.

species determined using the CPMG sequence (with hard pulses) were 1900, 480 and 29 ms for water, octanol and glycerol, respectively. In summary, the estimate of $T_2$ of each species obtained in our analysis gives $T_2$ values 10% higher than those obtained using a CPMG sequence for water and octanol, with better agreement for glycerol. However it is noted that our estimate of $T_2$ for glycerol is based on only on 2–3 points and therefore is subject to considerable experimental error.

### 3.2. Single-phase flow in a narrow tube

The 16 images acquired at a flow rate of $8\,\mathrm{ml\,min^{-1}}$ are shown in Fig. 4. In this implementation of the SEMI-RARE pulse sequence, Bloch decay signal from any pulse other than the initial excitation pulse will not be refocused as this magnetisation is not returned to the centre-line of **k**-space and so Bloch decay signal will be spoiled. Since signal is only derived from spins that are initially in the coil and received the initial excitation, fluid that moves into the coil after excitation will not contribute towards the signal and will appear as dark regions in the image. Thus, as seen in Fig. 4, the time-series of images form a multiple 'time-of-flight' measurement. Low intensity regions (propagating through successive images) correspond to fluid that was not in the coil and therefore not excited at the start of the pulse sequence. The images shown in Fig. 4 were gated, using the method described earlier, to discriminate between pixels containing signal from fluid which had been subject to the initial r.f. excitation, and fluid associated with zero signal, which had flowed into the field-of-view during the course of the experiment and which had therefore not been exposed to the r.f. excitation.

Given that the effective echo time for each image is known (taken as the mid-point of the data acquisition time for that image), the position of the interface across the tube diameter obtained from the image analysis allows calculation of the velocity of the fluid at each radial position across the narrow tube. For the flow rate and corresponding Reynolds number of 60 considered here, fully developed parabolic flow is expected at a distance of many tube diameters (>100) along the length of the tube. Under these conditions it can be shown using a simple force balance that the centre-line velocity should be double the average flow velocity; i.e., for fully developed laminar flow in a pipe, the velocity, $u$, at radius, $r$, should take the form:

$$u = 2u_m\left(1 - \frac{r^2}{a^2}\right), \tag{2}$$

where $u_m$ is the mean velocity and $a$ is the pipe radius. Therefore, given our experimental set-up, confirmation of the quantitative nature of the data obtained from application of the SEMI-RARE pulse will be demonstrated if the position of the moving front in the images shown in Fig. 4 is consistent with Eq. (2). Velocity profiles for images 5, 6, 7, and 8 in Fig. 4 are shown in Fig. 5 along with fits of Eq. (2) through the data points extracted from each image. In all cases the fit to the profiles produces a (maximum) centreline velocity to within 3% of the experimental centreline velocity of $40.3\,\mathrm{mm\,s^{-1}}$ as calculated from the volumetric flow rate and Eq. (2). The excellent agreement between the ex-

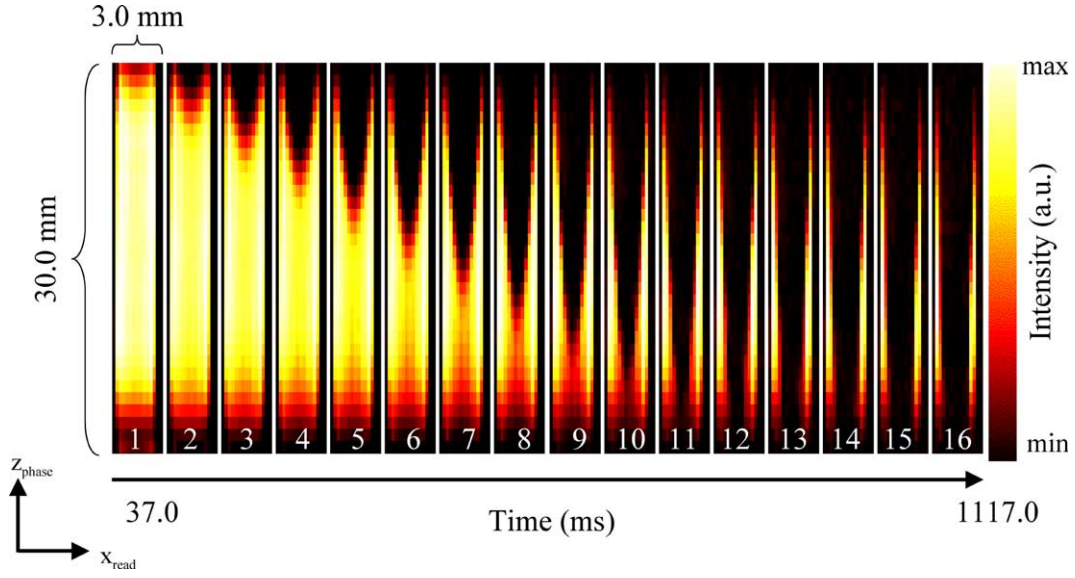


Fig. 4. Sixteen successive SEMI-RARE $zx$ images of single-phase liquid flow along a tube of inner diameter 2.9 mm. The development of a parabolic profile is clearly visible in the series of images. The images are equivalent to a multi-image 'time-of-flight' measurement. The liquid flow rate was $8\,\mathrm{ml\,min^{-1}}$.

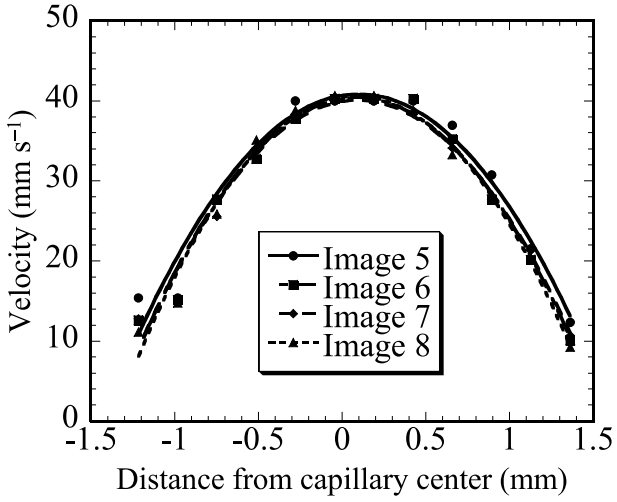


Fig. 5. Fits of Eq. (2) to the data extracted from Fig. 4. Excellent agreement between experimental data and theoretical prediction is seen.

perimental data and the prediction of Eq. (2) confirms that the SEMI-RARE time-of-flight data provide a quantitative characterisation of the flow. Further, the agreement with the analytical result confirms that the binary-gating process used and the assignment of a single image 'time' (the image 'time' being the mid-point of the data acquisition time for a given image) with a specific position of the boundary between fluid that had or had not been exposed to the initial excitation pulse avoids any mis-registration effects.

### 3.3. Two-phase flow in a narrow tube

A series of 8 images acquired following a single r.f. excitation are shown in Fig. 6. The first of these clearly shows a liquid slug close to the centre of the field-of-view. The curvature of the interface caused by surface tension effects is clearly seen; air bubbles above and below the slug have rounded ends reducing the gas/liquid interfacial area. Surface wetting of the tube adjacent to air bubbles is evident just above the noise level. At increasing image number (and corresponding effective echo time) the liquid slug moves down the tube. It is seen that while the signal close to the walls of the tube and at the leading edge of the slug decays gradually throughout the image sequence; the loss of signal at the trailing edge of the slug is far more significant. Further, this signal attenuation extends further into the liquid slug from the trailing edge, with successive images. We suggest that this attenuation of signal intensity arises from liquid recirculation in the

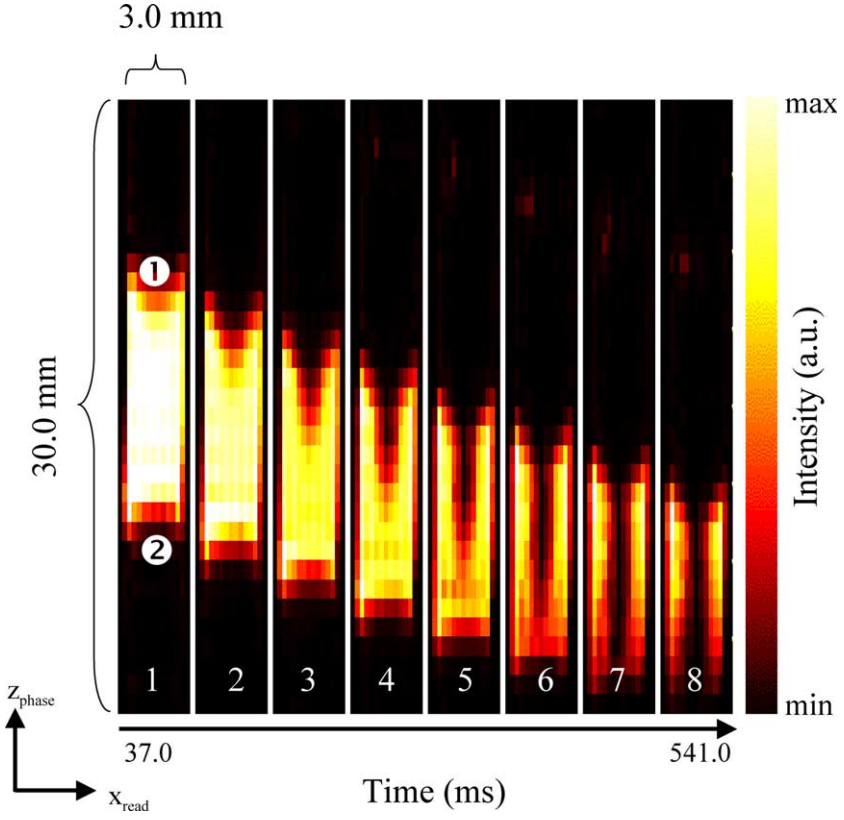


Fig. 6. Eight successive SEMI-RARE *zx* images of bubble-train flow along a tube of inner diameter 2.9 mm, with equal gas and liquid flow rates, each of approximately 4.0 ml min$^{-1}$. The overall movement of the bubble is clearly seen, along with increasing signal loss towards the centre of the bubble due to recirculation within the liquid slug. The trailing (1) and leading (2) edges of the liquid slug are identified.

liquid slug, consistent with the studies of Thulasidas et al. [5,6]. The cumulative loss of signal from the trailing edge of the liquid slug seen in region 1, as identified in Fig. 6, is a result of unexcited *extra*-slice magnetisation entering the slice-selective plane during the image acquisition. The flow profile at both the trailing and leading edges of the liquid slug is torodial in nature [6] and initially unexcited liquid from outside the imaging slice will therefore move into the slice-selective plane, becoming apparent as dark regions in the image, as time proceeds. These unexcited spins will migrate towards the leading edge of the slug as the liquid re-circulates, thereby causing signal loss. Because of the toroidal nature of the re-circulation patterns, fluid at the leading edge of the slug will migrate towards the walls (often outside the slice, in which case coherent signal will not be recovered) and will be replaced by fluid from just behind the leading edge, i.e., fluid that is already in the excited slice. Therefore at the leading edge of the liquid slug, any liquid re-circulation merely replaces excited spins leaving the image plane with excited spins originating from inside the image plane. This motion artefact is cumulative and therefore explains the asymmetric loss of signal, between the trailing and leading edges, along the length of the liquid slug. A simple analysis assuming that the fluid adjacent to the wall moves to the centre of the slug during flow along the tube, consistent with toroidal recirculation, was performed. Since the profile of the excitation pulse is known, the initial transverse magnetisation adjacent to the wall of the tube at the beginning of the sequence can be calculated and compared to the maximum theoretical transverse magnetisation, i.e., where all the fluid adjacent to the wall has been fully excited. For the Gaussian excitation pulse used here with a full width at half maximum corresponding to the slice thickness, the fraction of total magnetisation adjacent to the walls transferred to the transverse plane is 1/8th. If all of this fluid then moves to the centre of the tube, the signal from the dark region at the centre of the tube is expected to be approximately 1/8th that from fluid near the walls which has not moved into/out of the slice. Experimentally this value is found to be closer to 1/7th but, given the assumptions made in the analysis which include neglect of any mixing effects due to diffusion, our observations appear consistent with this explanation.

The effect of magnetic susceptibility artefacts on the acquired data has also been considered. First, the experiment is designed such that the direction of the flow, in which we wish to acquire quantitative information, is in the phase direction thereby minimising any effects of susceptibility in the acquired data. Second, the effect of magnetic susceptibility artefacts which may occur in the read direction is reduced in this experiment by employing a high bandwidth (150 kHz over 64 pixels). These two features of the experimental design ensure that the effect of magnetic susceptibility on the data is negligible in the phase direction and minimised in the read direction. Confirmation that magnetic susceptibility artefacts and mis-registration effects have negligible effect on the quantitative nature of the data obtained is achieved by calculating the average velocity of the liquid slug within the image. For the data shown in Fig. 6, the average velocity of the slug over the 8 image series is obtained by monitoring the position of the trailing edge of the liquid slug with time (this is possible since there is no recirculation artefact at the walls of the tube), and is found to be $22\,\mathrm{mm\,s^{-1}}$. This is in good agreement with the measured average liquid velocity of $20 \pm 4\,\mathrm{mm\,s^{-1}}$ based on the overall gas and liquid flow rate.

### 3.4. Mis-registration effects

The effect of boundary mis-registration within a single image needs to be considered for the cases of both single- and two-phase flow. Mis-registration errors may arise due to the fact that a finite period of time is required for image acquisition. During this time, the boundary to be identified in the experiment (i.e., excited/non-excited fluid in the single-phase flow experiment, and the gas–liquid boundary in the two-phase experiment) moves and therefore the image must contain some blurring of the position of the interface. In our analyses, we identify the 'time' associated with a given image as the mid-point of the data acquisition time for that image. As discussed earlier, the algorithm used to identify the appropriate interface at this 'time' identifies the position at the mid-point in the signal intensity acquired in the image. The reasons for this and the errors introduced into our analysis are discussed below, using the images of two-phase flow as our example. Similar arguments follow for the case of single-phase flow although the blurring of the interface is less obvious because of the less sharp interface between regions containing signal and no signal.

Considering the data shown in Fig. 6, the liquid slug moves a significant distance, up to 10% of the field-of-view, over the duration of each image acquisition. Hence, it may be asked at what point in time should the interface we identify be assigned? To answer this question, simulations have been performed in which a Fourier domain data set is constructed from a moving (real space) step function; the influence of partial volume effects and hence the non-ideality of the step function has been considered in this analysis. Time domain data were generated for movement of the interface through 32 time steps, each corresponding to a particular value of $\mathbf{k}_{\mathrm{phase}}$. In-between each generation of a Fourier domain complex data point the step function was moved by a distance such that the step moved a total of 12.5% (4 pixels)

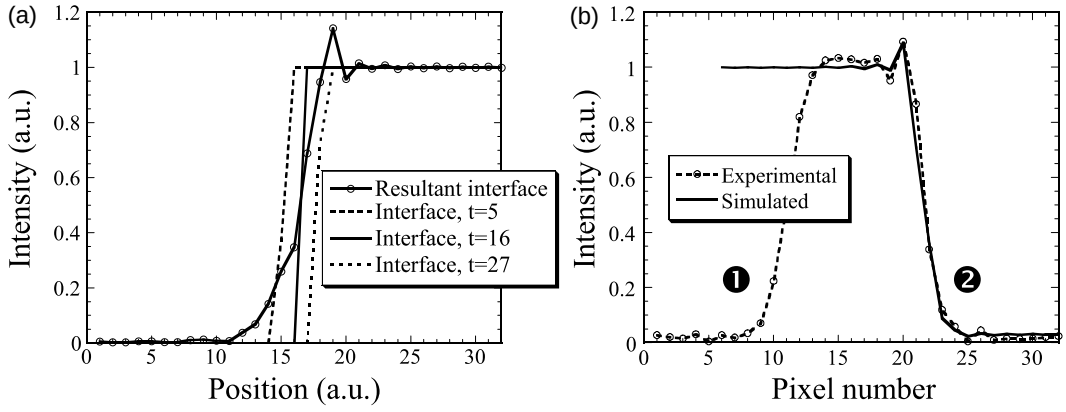


Fig. 7. (a) The position of a model interface (i.e., step function) at three different time steps during a simulated data acquisition process is shown. For comparison the predicted signal intensity associated with such a moving interface is also shown. This has been calculated by reverse Fourier transform of the input function at 32 positions (i.e., time steps), each one corresponding to an increment of the phase gradient. (b) Comparison of signal intensity along the centreline ($z$-direction) of the liquid slug shown in Fig. 6 (Image 1), with the prediction of the simulation. The leading and trailing edge of the liquid slug are identified as in Fig. 6. The oscillation to the high intensity side of the 'step' in image intensity is only seen at the leading edge in the experimental data because of the signal loss at the trailing edge assigned to liquid recirculation phenomena.

of the entire field-of-view during the complete simulation, thereby representing a worst-case scenario in the experimental data acquisition. Fig. 7a shows the position of the moving interface (i.e., step function) at three time points in the simulation. Also shown is the result of the reverse Fourier transform obtained from all 32 time steps in the simulation. The form of the reverse Fourier transform shows that the effect of motion of the interface during image acquisition is to produce a blurring of the interface in the acquired image, with a decaying oscillation at the high intensity edge of the interface. It is seen that if the gating level is chosen at the mid-point in the signal intensity, the position of the 'step' in the recovered function always occurs at the position at which the input step function exists at the time when the central $\boldsymbol{k}$-space point is acquired. The 'time' assigned to each image, gated using the present algorithm, is therefore correctly taken to be the time at which the central value of the phase gradient ramp is applied; i.e., when we sample $\mathbf{k}_{\text{phase}} = 0$.

To confirm the validity of this approach, Fig. 7b shows a comparison of the signal intensity variation along the centre line ($z$-direction) of the liquid slug within the tube, with the numerical prediction. The experimental data have been taken from Fig. 6, Image 1. To achieve this comparison, the velocity of the interface used as input to the simulation has been taken directly from the experimental data. The agreement is good with respect to both the blurring of the interface and the decaying oscillation at the high intensity side of the interface; i.e., the leading edge of the liquid slug. It is noted that if a different gradient scheme is used (e.g., if the first point in time is at $\mathbf{k}_{\text{phase}} = 0$ and the phase gradient is ramped to a maximum and then from negative maximum up to $\mathbf{k}_{\text{phase}} = 0$ again), a more complex analysis of the data may be required.

## 4. Conclusions

Single excitation multiple image RARE, SEMI-RARE, has been used to produce multiple high-resolution $^1$H images for a single excitation pulse, using a 7.07 T microimaging MRI spectrometer. 120 successive image acquisitions have been acquired of a static phantom following a single 90° excitation pulse. The ability of a sequence of SEMI-RARE images to discriminate between components within the image on the basis of differing relaxation times and self-diffusion coefficients is demonstrated, and the effects of relaxation and diffusion contrast on the quantitative nature of the images is addressed.

For the case of single- and multi-phase flows within a single narrow tube, successive image acquisitions are more typically limited to 8–16 as a result of the residence time of the fluid in the coil and other motion effects. The quantitative nature of the data obtained is confirmed by showing that a parabolic flow profile is obtained directly from the images of single-phase flow with a measurement of the centreline velocity to within 3% of the theoretical value. We then demonstrate the ability of SEMI-RARE to record a series of 8 images of two-phase bubble-train flow from a single r.f. excitation. From these images the bubble-size and velocity can readily be obtained, and we suggest that the data presented also provide the first magnetic resonance observation of liquid recirculation in bubble-train flow.

The data presented suggest that the robustness of the SEMI-RARE technique makes it an attractive fast imaging technique for the study of multi-phase flow phenomena, which are often characterised by large variations in magnetic susceptibility, and are of widespread interest in chemical and reaction engineering.

## Acknowledgments

AJS acknowledges EPSRC for financial support. LFG wishes to thank EPSRC for the award of the NMR spectrometer.

## References

[1] J. Hennig, A. Nauerth, H. Friedburg, RARE imaging—a fast imaging method for clinical MR, Magn. Reson. Med. 3 (1986) 823–833.
[2] D.N. Guilfoyle, P. Mansfield, K.J. Packer, Fluid flow measurement in porous media by echo-planar imaging, J. Magn. Reson. 97 (1992) 342–358.
[3] A.M. Peters, P.S. Robyr, R.W. Bowtell, P. Mansfield, Echo-planar microscopy of porous rocks, Magn. Reson. Imag. 14 (1996) 875–877.
[4] B. Manz, P.S. Chow, L.F. Gladden, Echo-planar imaging of porous media at spatial resolution below 100 μm, J. Magn. Reson. 136 (1999) 226–230.
[5] T.C. Thulasidas, M.A. Abraham, R.L. Cerro, Bubble train flow in capillaries of circular and square cross section, Chem. Eng. Sci. 50 (1995) 183–199.
[6] T.C. Thulasidas, M.A. Abraham, R.L. Cerro, Flow patterns in liquid slugs during bubble train flow inside liquid capillaries, Chem. Eng. Sci. 52 (1997) 2947–2962.
[7] J. Hennig, k-space sampling strategies, Eur. Radiol. 9 (1999) 1020–1031.
[8] H. Bosmans, S. Gryspeerdt, L. Van Hoe, S. Van Oostende, T. De Jaegere, B. Kiefer, A.L. Baert, G. Marchal, Preliminary experience with a new double-echo half-Fourier single-shot turbo spin echo acquisition in the characterisation of liver lesions, Magn. Reson. Mater. Phys. 5 (1997) 79–84.
[9] B. Kiefer, J. Grassner, R. Hausman, Image acquisition in a second with half-Fourier acquisition single-shot turbo spin-echo, J. Magn. Reson. Imag. 4 (1994) 86–87.
[10] T. Miyazaki, Y. Yamashita, T. Tsuchigame, H. Yamamoto, J. Urata, M. Takahashi, MR cholangiopancreatography using HASTE (half-Fourier acquisition single-shot turbo spin-echo) sequences, Am. J. Roentgenol. 166 (1996) 1297–1303.
[11] M.D. Mantle, A.J. Sederman, S. Raymahasay, E.H. Stitt, J.M. Winterbottom, L.F. Gladden, Dynamic MRI visualisation of two-phase flow in a ceramic monolith, AIChE J. 48 (2002) 909–912.
[12] A. Haase, J. Frahm, D. Matthaei, W. Hanicke, K.D. Merboldt, FLASH imaging—rapid NMR imaging using low flip-angle pulses, J. Magn. Reson. 67 (1986) 258–266.
[13] A. Oppelt, R. Graumann, H. Barfuss, H. Fischer, W. Hartl, W. Shajor, FISP—a new fast MRI sequence, Electromedica 54 (1986) 15–18.
[14] P.T. Callaghan, Principles of Nuclear Magnetic Resonance Microscopy, Clarendon Press, Oxford, 1991.
[15] D.G. Norris, P. Bornert, T. Reese, D. Leibfritz, On the application of ultra-fast RARE experiments, Magn. Reson. Med. 27 (1992) 142–164.
[16] J. Hennig, Multiecho imaging sequences with low refocusing flip angles, J. Magn. Reson. 78 (1988) 397–407.
[17] S. Majumdar, Errors in the measurements of $T_2$ using multiple-echo MRI techniques. 1. Effects of radiofrequency pulse imperfections, Magn. Reson. Med. 3 (1986) 397–417.
[18] A.M. Peters, R. Bowtell, Resolution in high field echo planar microscopy, J. Magn. Reson. 137 (1999) 196–205.
[19] Bruker Almanac, Bruker Biospin Ltd, 2002, p. 72.